Electrical Power System Resilience Assessment: A Comprehensive Approach

Hamed Sabouhi, Aref Doroudi, Mahmud Fotuhi-Firuzabad, *Fellow, IEEE*, and Mahdi Bashiri

***Abstract*—Extreme weather events such as earthquake and hurricane have disastrous consequences on power systems. Due to the inherent nature of these events, as high-impact low-probability (HILP) events, selection of an appropriate method that can provide the effects of weather conditions on the power system behavior still remains a significant challenge. Resilience is a new concept that focuses on mitigating the destructive effects of such disastrous events on power systems. This article provides a fundamental framework for quantifying and modeling of power systems resilience, with focus on high wind incidence. The algorithm composes of four steps. In the first step, the prerequisites of the analysis are described. Disaster modeling is carried out in step second and the transmission line status and system topology obtaining are outlined in the third step. In the last step, based on optimal power flow tracing, a novel resilience index is introduced based on axiomatic design concepts. The core of the main algorithm involves a novel matrix-based approach to count automatically all possible routes from generators to loads, considering load importance, before and after a disruption. The effectiveness of the proposed approach is illustrated by the IEEE 14-bus system. The proposed methodology is original and a comprehensive approach.**

***Index Terms*—Axiomatic design concept, high-impact low-probability (HILP), load importance, power system resilience.**

NOMENCLATURE

A, B	Assets and busbars.
CA,TA	Conversion and transmission assets.
$\text{CM}_{C_n}, \text{CM}_{T_n}$	Nonsequential constructional conversion and transmission grid constraint matrix.
CM_C, CM_T	Conversion and transmission grid constraint matrix (CGCM and TGCM).
$\text{CM}_{n\_s}, \text{CM}_s$	Nonsequential and sequential constructional grid constraint matrix (NSCGCM and SCGCM).
$\text{CPM}_i, \text{TPM}_i$	Delivery of service conversion and transmission possibility matrix (DOSCPM and DOSTPM) for delivery of service i.
$\text{CQOF}_{n\_s}, \text{CQOF}_s$	The nonsequential and sequential constructional quantity of freedom.
DOS_j	Delivery of service j.
$F_L(w_i), F_T(w_i)$	Line and tower failure probability.
$LC_i(\upsilon_1, \upsilon_2)$	Delivering power for delivery of service i.
$LC_{i0}(\upsilon_1, \upsilon_2)$	Delivering power to load for delivery of service i in normal operation.
p	Number of feasible paths.
RI	Resilience index.
$\text{RM}_{C_{n\_s}}, \text{RM}_{T_{n\_s}}$	Nonsequential constructional conversion and transmission grid relation matrix (NSCCGRM and NSCTGRM).
RM_C, RM_T	Conversion and transmission grid relation matrix (CGRM and TGRM).
$\text{RM}_{n\_s}, \text{RM}_s$	Nonsequential and sequential constructional grid relation matrix (NSCGRM and SCGRM).
RT_i	Repair time.
$\text{SE}_{C_{xi}}, \text{SE}_{T_i}$	Conversion and transmission service event matrix for delivery of service i.
SE_{xi}	Conversion and transmission service event matrix for delivery of service i.
$\text{SE\_}C_{xi}, \text{SE\_}T_i$	Conversion and transmission service event matrix for delivery of service i.
se_x	Service events.
$SM_{CT_{xi}}$	Sequential constructional grid relation matrix-conversion, transmission for delivery of service i.
SM_i	Sequential constructional grid relation matrix (SCGRM) for delivery of service i.
SM_{i0}	Sequential constructional grid relation matrix for normal operation.
$SM_{TC_{(x+1)i}}$	Sequential constructional grid relation matrix-transmission, conversion for delivery of service i.
SM_{TT_i}	Sequential constructional grid relation matrix—two successive transmissions for delivery of service i.
W_i, W_j	Weighing factor of each load and generator for delivery of service i.
W_{i0}	Weighing factor of each load for delivery of service i in normal operation.
λ_i, μ_i	Failure rate and repair rate of component i.

Manuscript received December 9, 2018; revised April 9, 2019 and July 3, 2019; accepted August 5, 2019. Date of publication September 9, 2019; date of current version June 3, 2020. *(Corresponding author: Aref Doroudi.)*

H. Sabouhi and A. Doroudi are with the Department of Electrical Engineering, Shahed University, Tehran 3319118651, Iran (e-mail: hamed.sabouhi@shahed.ac.ir; Doroudi@shahed.ac.ir).

M. Fotuhi-Firuzabad is with Center of Excellence in Power System Management and Control, Department of Electrical Engineering, Sharif University of Technology, Tehran 11155-1639, Iran (e-mail: fotuhi@sharif.edu).

M. Bashiri is with the Department of Industrial Engineering, Shahed University, Tehran 3319118651, Iran (e-mail: Bashiri@shahed.ac.ir).

Digital Object Identifier 10.1109/JSYST.2019.2934421

I. Introduction

ELECTRICAL energy is one of the most important needs of modern societies. All societies have tried to generate and transfer more energy with low cost and high reliability. Power grids are responsible for transferring of electrical energy from power plants to the electrical loads and are always exposed to severe environmental conditions, such as earthquake, hurricane, flood, etc. [1]–[4]. Severe weather in United States which led to 58% power grid outages between 2003 and 2012, the 2011 earthquake and tsunami in Japan, the 2010 earthquake in Haiti, and the 2005 hurricanes in the U.S. Gulf of Mexico are examples of such disasters [5]. In the US–Canada Task Force report [1], the cascading failures caused great social and economic damages. These HILP events mostly result in power grid outages and imposition of heavy financial losses.

Traditional reliability methods measure the performance of system supplying power to all connected loads. These methods do not take into consideration the origins of events and also do not attribute to HILP events. Consequently, it is necessary to define a new concept for preventing or mitigating the impact of natural disasters. Studies in this field have led to the emergence of a novel concept called grid resilience. The concept of resilience was first raised in psychology [6]. The resilience expresses the ability of an equipment or a system (or a person) to return to normal conditions after a major disruption. This concept is divided into two main categories of static and dynamic. Static resilience measures the performance of a system after a disruption and it is independent of time while a dynamic resilience examines how quickly a system recovers to the normal operation. Some of the specific power network principles, such as absorption, physical redundancy, reduce complexity, reorganization, repairability, localized capacity, and loose coupling can be included in the resilience analysis [7]. In this article, the absorption principle was emphasized. Actually, this principle implies that the system shall be capable of absorbing the magnitude of the disruption that it encounters.

To quantify the resilience concept, various indices are presented so far. Generally, four crucial steps are employed to obtain these indices, which are as follows:

1) Step 1: fulfilling data requirements (e.g., wind profiles);
2) Step 2: disaster modeling;
3) Step 3: equipment status and system topology determination;
4) Step 4: introducing a resilience index (RI).

In recent years, several resilience studies which were carried out only considered weather-related incidents (steps 1 and 2) involving severe thunderstorms, hurricanes, and earthquakes [8]. Evaluating the impact of extreme weather events on power systems has also attracted several researchers [9], [10]. These articles concentrated on the hardening and strengthen activities such as construction of a redundant route or design change of power system components. Due to nature of extreme weather events, the indices proposed in these articles are not able to give useful information about the operational resilience measures. After modeling of weather-related events, it is necessary to quantify and anticipate the impact of weather events on network topology (step 3). Billinton [11] have highlighted the importance of employing two adverse weather states, when modeling transmission line failures by Markov processes. The method is then developed to three [12] and four adverse weather states [13] to increase the accuracy of the weather modeling. Because of their complexity, these methods can be only employed in small grids. However, by increasing the scale and interconnectivity of modern power grids, it is necessary to predict the weather-related outage of a whole power system as a function of time-dependent and independent variables. The predicted outages can be mainly obtained with the statistical regression-based models such as accelerated failure time (AFT) [14], multivariate adaptive regression splines [15], and Cox proportional hazards model (Cox PHM) [16].

After a suitable weather model is found, it is necessary to introduce a proper index to measure systems resilience (step 4). There can be found many references devoted to the evaluation of systems resilience in the psychology, environmental, social, and organizational fields [17], [18]. The resilience concept is approximately new in the engineering domain in comparison to other fields. A novel stochastic network design formulation for maximizing travel time resilience for roadway networks is introduced in [19]. The article addressed the three stages of decision processes of the disaster management life cycle, specifically pre-event mitigation and preparedness, and postevent response. The problem of assessing and maximizing the resilience of an airport's runway and taxiway networks under multiple potential damage-meteorological scenarios has been conceptualized and mathematically formulated as a two-stage stochastic integer program in [20]. The main purpose is to quickly restore postevent takeoff and landing capacities to pre-event operational levels taking into account budgetary, time, space, and physical resource limitations. Pant *et al*. [21] introduced a new multidimensional resilience function that allow multiple resource allocation scenarios where the static and dynamic resilience indices are proposed that confirm to well-known resilience concepts of robustness, rapidity, redundancy, and resourcefulness. A general metric for quantifying resilience for complex systems as a relationship of system performance against time has been presented in [22]. The article described a new model and visual tools that develop capabilities to determine the resilience behavior of complex systems.

In power systems context, some reliability indices such as loss of load frequency, loss of load expectation, and expected energy not supplied have been employed as a resilience index [23]–[25]. More recently, some other indices have been proposed for power system resilience evaluation. The resilience index that has been presented in [26] is the mismatch between dispatched power and actual power generated at a specific time throughout the system. Panteli *et al*. [27] measured the grid resilience by a severity risk index to reduce the cascading failures. Farzin *et al*. [28] proposed a new resilience index, which can measure the effectiveness of the proposed outage management scheme in terms of the expected energy curtailment during a disturbance.

In addition to the abovementioned indices, valuable efforts have been devoted to provide traditional graph theory metrics for assessing the grid resilience from a topological point of

view [29], [30]. However, finding a comprehensive resilience index for power grids is still a challenging research issue. Some other resilience indices can be found in [31]–[33] for interested readers.

In this article, a novel and comprehensive grid resilience assessment framework is proposed from a topological perspective. A four-step straightforward approach is presented where in the first step, the prerequisite and the required data for disaster modeling are introduced. With focus on wind events, the required data are the regional wind speed profiles in the different regions of the studied grid and the associated reliability data. Disaster modeling is demonstrated in the second step. The process is followed by the impact modeling of severe weather conditions on power grids. The impact is modeled by the fragility curve based on reliability data and using the Monte Carlo simulations method. The last step suggests a novel systematic resilience matrix-based index. The novel index is used based upon an axiomatic design concept, which is a systematic binary matrix approach to numerically present the large flexible engineering systems such as production systems, transportation, and water distribution networks. The new index systematically enumerates the feasible paths from sources to destinations based on dc optimal power flow and axiomatic design concept. In summary, main contributions of this article are as follows.

1) This article introduces a full systematic binary matrix representation for power system apparatus and subsystems. Adding or removing equipment to and from power networks and any remedial actions can be easily implemented by this approach.
2) It suggests a novel and comprehensive grid resilience assessment framework from a topological point of view. It can be applied to all types of power networks.
3) This article provides a novel resilience index for power grids. It can precisely show the grid status during severe weather conditions. The index can also easily reflect any remedial actions and can be used for comparison of networks from the resilience point of view.
4) Because of binary matrices used in the algorithm, the proposed index can be so efficient for optimization problems.
5) The proposed algorithm considers loads priority, which is an important feature of power systems during assessment of the grid resilience. The loads priority can change power flow routes and consequently the network resilience.

The rest of the article is organized as follows. Section II presents the proposed resilience evaluation framework. The proposed index is calculated in Section III using simulations on the IEEE 14-bus power system. The concluding remarks of this article are given in Section IV.

II. Power Grid Resilience Evaluation Framework

Hollnagel [34] states that "resilience is the ability to maintain effective barriers that can withstand the impact of adverse agents and the erosion that is a result of latent conditions." In general, resilience indices determine the system resiliency by comparing the performance of a system before and after disruptions without focusing on specific system features. The indices can be divided into two major groups of deterministic and stochastic [35], [36]. The deterministic indices do not consider uncertainties in the measuring, whereas the stochastic indices take into account the probabilistic and random behavior of the system.

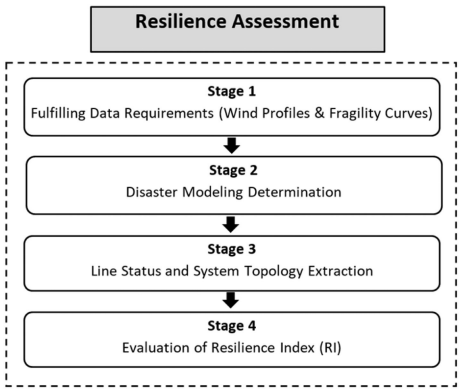

Fig. 1. General framework for resilience assessment.

The framework of resilience assessment is shown in Fig. 1. The algorithm is comprised of four steps as fulfilling data requirements, disaster modeling, line status and system topology determination, and evaluation of resilience index. This structure comprehensively covers all the requisite procedures and outcomes from technical views.

A. Fulfilling Data Requirements for Disaster Modeling

In this step, all data required for the disaster modeling, with focus on wind events including wind speed profile and reliability data associated with the transmission lines and towers are prepared. The reliability analysis involves sufficient valid data collection on the technical features of power network components. The reliability data have been collected from outage reports in a sufficient and valid data format for lines and towers. The time-series regional wind profiles are obtained using recorded statistical data from wind speed at the meteorological station. For this purpose, wind profiles for several years with an hourly time resolution are generated, and then a three days, hourly wind profile is randomly selected among this. These wind profiles were generated at different regions, and the wind profile with the maximum wind speeds were then chosen. The hourly wind profiles are finally scaled up [37], [38].

The fragility curve-based modeling is generally used for assessment of the impact of severe weather conditions on transmission lines and towers. A fragility function describes the failure probability of a structure, which depends on a loading that relates the potential severity of a hazard [39]. All the fragility curves are in the form of lognormal cumulative distribution functions, defined in terms of the logarithmic mean and the logarithmic standard deviation. Fragility curve can be obtained by five ways including experimental, empirical, analytical, expert judgment, and combination of these methods. Because of the insufficient and uncertain wind-related failure data, analytical methods are the best approaches for obtaining the failure probability of structural components. These methods employ a structural simulation model [33]. In order to construct the tower fragility

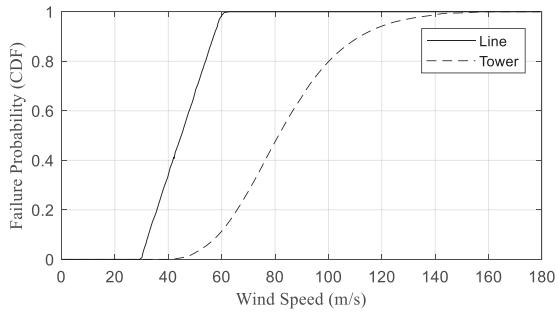

Fig. 2. Wind fragility curves related to the transmission lines and towers.

curve, material and geometrical nonlinearities under different range of wind speed, should be analyzed. For transmission lines, the empirical statistical data could help to develop the fragility curve. Fig. 2 illustrates the general fragility curve that relates the failure probability of the lines and towers to the wind speed. According to this curve, the impact of wind speeds on the operational state of lines and towers can be determined.

B. Line Status and System Topology Determination

In order to determine the status of transmission lines and towers under various weather conditions, the fragility curves (based on reliability data) and Monte Carlo simulations method are employed. The procedure is as follows.

1) Step 1: Determine wind speed information at different regions based on hourly regional wind profiles (w_i).
2) Step 2: Compute lines and towers failure probability (wind intensity) based on wind fragility curve according to

$$F_L(w_i) = \begin{cases} 1 - \exp(\lambda_L t) & \text{if } w_i < w_{\text{critical}} \\ F_L(w_i) & \text{if } w_{\text{critical}} \pounds w_i < w_{\text{collapse}} \\ 1 & \text{if } {w_i}^3 w_{\text{collapse}} \end{cases} \tag{1}$$

$$F_T(w_i) = \begin{cases} 0 & \text{if } w_i < w_{\text{critical}} \\ F_T(w_i) & \text{if } w_{\text{critical}} \le w_i < w_{\text{collapse}} \\ 1 & \text{if } \ w_i \ge w_{\text{collapse}} \end{cases} \tag{2}$$

where $F_L(w_i)$ and $F_T(w_i)$ describe, respectively, transmission line and tower failure probability as a function of wind speed, λ_L is the "good weather conditions" failure rate, w_{critical} is the wind speed at which the network component's failure probability picks up, and w_{collapse} is the wind speed at which the component has a negligible probability of survival. In this article, w_{critical} and w_{collapse} are considered 30 m/s and 60 m/s, respectively, for lines. For towers, these parameters are assumed as 45 m/s and 150 m/s, respectively [40].

3) Step 3: Estimate failure patterns and outage durations of equipment using a sequential Monte Carlo Simulation method [41]. For all of the components, uniform distributed random numbers between [0, 1] (rand_i) are generated, and compared with the failure probabilities (i.e., $F_L(w_i)$ and $F_T(w_i)$) for each hour. If $F_L(w_i) > \text{rand}_i$, a transmission line outage occurs (3). If $F_T(w_i) > \text{rand}_i$, the tower collapses. Single or double circuits' outage may happen due to this type of failure (4)

$$\text{Transmission line outage} = \begin{cases} 0 & \text{if } F_L(w_i) < \text{rand}_i \\ 1 & \text{if } F_L(w_i) > \text{rand}_i \end{cases} \tag{3}$$

$$\text{tower outage} = \begin{cases} 0 & \text{if } F_T(w_i) < \text{rand}_i \\ 1 & \text{if } F_T(w_i) > \text{rand}_i. \end{cases} \tag{4}$$

After a line or tower outage, the repair time (RT) can be calculated chronologically using

$$\text{RT}_i = -\frac{1}{\mu_i}\ln(1-R) \tag{5}$$

where R is a uniformly distributed random number and μ_i is the repair rate. It is worth noting that RT of transmission lines and towers are different. As it is obvious, the RT of equipment can increase at higher wind speeds. So, in this article, the three damage levels are defined: low $(w_i \le 20\ \text{m/s})$, medium $(20\ \text{m/s} \le w_i \le 40\ \text{m/s})$, and severe $(w_i > 40\ \text{m/s})$ and RT is determined as the following equation under these conditions:

$$\begin{aligned} \text{RT}_i &= -\frac{1}{\mu_i}\ln(1-R) \\ &= \begin{cases} 1-e^{-1} \le R < 1-e^{-3}; & \text{if } w_i \le 20\,\text{m/s} \\ 1-e^{-3} \le R < 1-e^{-5}; & \text{if } 20\,\text{m/s} < w_i \le 40\,\text{m/s} \\ 1-e^{-5} \le R < 1-e^{-7}; & \text{if } w_i > 40\,\text{m/s}. \end{cases} \end{aligned} \tag{6}$$

Indeed, a random value within a predetermined range is multiplied to repair time for each level.

4) Step 4: Repeat steps 2 and 3 in a given time period. Update the state of all transmission lines based on the derived failure and repair patterns and their wind-affected operational state.
5) Step 5: Update the number of Monte Carlo samples $i_{\text{MCS}} = i_{\text{MCS}} + 1$ and repeat steps 1–4. The inherent uncertainty in the Monte Carlo method can be greatly reduced with a lot of samples.
6) Step 6: Use dc OPF as a dispatch tool. If priority of loads is considered, it is necessary to calculate the power contribution of each generator to each load using power flow study. This is done by dc OPF and the method has been proposed in [42].
7) Step 7: Record the change of power grid topology and components conditions caused by lines and towers failures.

The flowchart of the abovementioned algorithm is shown in Fig. 3.

It is worth noting that the complexity and loose coupling are also necessary taken into account in order to determine the effect of weather events on the status of equipment [43]. This article ignores those factors.

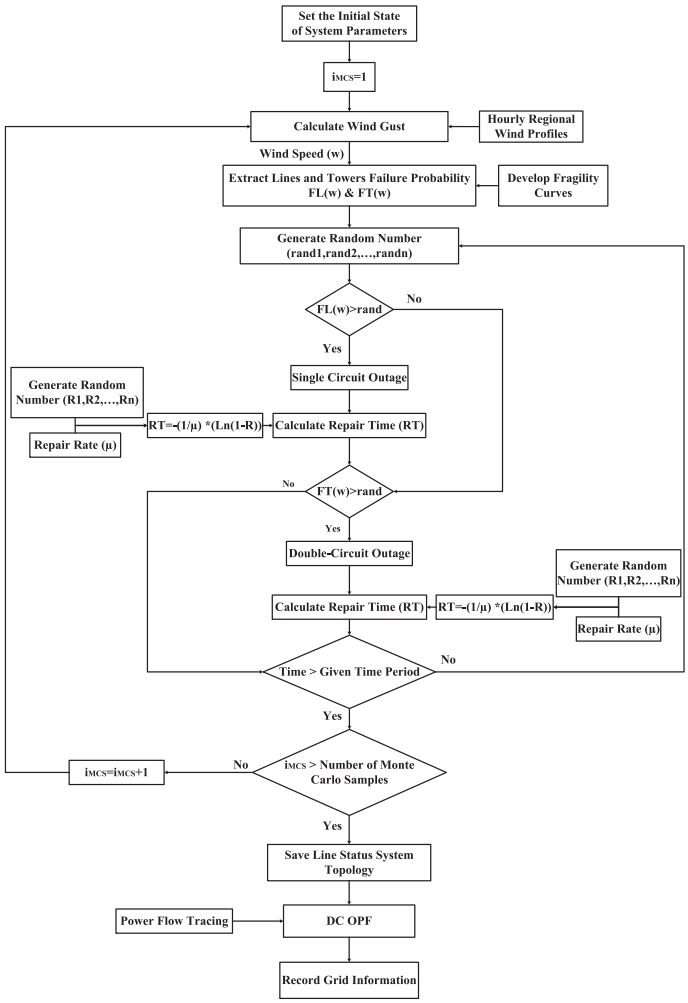

Fig. 3. Resilience evaluation algorithm.

C. Calculation of Axiomatic Design Concept Matrices

This section uses an axiomatic design concept matrix to present the proposed resilience index. Axiomatic design uses binary matrices to disengage parameter of the system's design from its functional requirements [44]. In this concept, two essential terms "design parameter" (asset) and "functional requirement" (process) are primarily defined.

Power grid assets (A) can be generally classified into three categories of conversion assets (CA), transmission assets (TA), and busbars (B). These assets can be presented as

$$A = \mathrm{CA} + \mathrm{TA} + B. \tag{7}$$

Conversion assets cover all components that convert energy from one form to another, whereas transmission assets include all components that handle the transmission of energy from one point to another. Generator and electrical loads are examples of conversion assets and overhead line is an example of transmission assets. Busbars usually are employed to make a common connection between several circuits in power grids.

Power grid processes can be also classified into two main categories of conversion processes and transmission processes. A conversion process converts energy from one form to another, whereas the transmission process transmits energy from one area to another. For example, compression, combustion, generation, and consumption are the types of conversion processes.

In axiomatic design concept, the binary matrix that describes power network design and structure is called as a relation matrix (RM). In fact, this matrix map a set of power grid processes to their assets. Two binary relation matrices can be defined as follows [45].

1) Conversion grid relation matrix (RM_C): This matrix shows the relation between conversion assets and their processes.
2) Transmission grid relation matrix (RM_T): This matrix shows association between transmission asset and its processes.

Each entry of these matrices is called an event that shows a feasible combination of a process and an asset.

In order to apply power grid constraints, constraint matrices with the same dimensions of the relation matrices should also be defined. By default, all entries of the constraint matrix are zero. To include the power network constraints such as targeted shooting of transformers, intentional downing of power lines or restriction of transmission of ac power into dc lines, it is only necessary to change the relevant entries of the constraint matrices from zero to one.

The abovementioned relation and constraint matrices can be combined to quantify the capabilities of power grids. For this purpose, constructional quantity of freedom (CQOF) that measures the capabilities of power grid assets is defined. The concept of CQOF was basically extracted on the basis of the mechanical degree of freedom. CQOF can be employed to describe delivery of service configuration of an electrical grid. By their dependence on the sequence of execution, the CQOF is classified into two categories: sequential and nonsequential. Sequential CQOF provides a sequence dependent measure of the capabilities, whereas nonsequential CQOF ignores the sequence.

1) Nonsequential CQOF: Nonsequential CQOF relinquishes sequence of its processes. In order to determine the nonsequential constructional grid RM (RM_{n_s}), conversion and transmission grid relation matrices should be combined together via [46]

$$\mathrm{RM}_{n\_s} = \left[\begin{array}{c|c} \mathrm{RM}_C & \mathbf{0} \\ \hline \mathrm{RM}_T & \end{array}\right]. \tag{8}$$

The nonsequential constructional grid constraint matrix (CM_{n_s}) can be also obtained with the same concept using

$$\mathrm{CM}_{n\_s} = \left[\begin{array}{c|c} \mathrm{CM}_C & \mathbf{1} \\ \hline \mathrm{CM}_T & \end{array}\right]. \tag{9}$$

The nonsequential CQOF can be then calculated via (10). Broadly speaking, the nonsequential CQOF measures the number of way that all of the processes may be executed

$$\mathrm{CQOF}_{n\_s} = \sum_{\vartheta=1}^{n(P)} \sum_{\sigma=1}^{n(A)} \left[\mathrm{RM}_{n\_s}(1 - \mathrm{CM}_{n\_s})\right] \tag{10}$$

where the operator $n()$ gives the size of a set.

2) Sequential CQOF: Sequential CQOF provides a sequential measure of capabilities in a power grid. A series of processes must be done sequentially so as to generate and deliver power to consumers. A matrix is required to display the sequence of specified executing processes. The sequential constructional grid relation matrix (RM_s) is a square binary matrix that shows the sequence of the processes and can be calculated as [47]

$$\mathrm{RM}_s = [\mathrm{RM}_{n\_s}(1-\mathrm{CM}_{n\_s})]^V [\mathrm{RM}_{n\_s}(1-\mathrm{CM}_{n\_s})]^{VT} \tag{11}$$

where $[]^V$ and $[]^T$ show matrix vectorization and transpose, respectively. When the sequential CQOF is calculated by (11), a number of "one" entries are generated, which are unwanted. They must be removed from the matrix. For this purpose, a sequential constructional grid constraint matrix (SCGCM) is defined. SCGCM (CM_s) is a binary matrix of size *n(P)* × *n(A)* whose entry is equal to one under the following conditions.

1) Two successive conversion's events do not occur at the same assets.
2) A transmission event does not follow a conversion event.
3) A conversion event does not follow a transmission event.
4) Two transmission events do not fall in at the same busbar.

Actually, SCGCM guarantees that the origin and the destination of two consecutive processes are matched together. Calculation of these minimal constraints has been proposed in [48]. The sequential CQOF can then be calculated as

$$\mathrm{CQOF}_s = \sum_{\rho 1=1}^{(n(P)\times(A))^2} \sum_{\rho 2=1}^{(n(P)\times(A))^2} [\mathrm{RM}_s(1-\mathrm{CM}_s)]. \tag{12}$$

Now, the abovementioned quantified power system capabilities should be related to the outputs (delivery of services). To do this, mathematical calculations are performed to determine the paths leading to these outputs. To begin, it is necessary to define "delivery of service (DOS)," "service event (SE)," and "delivery of service possibility (DOSP)."

Power system provides a set of DOSs that each DOS consists of a set of SE (se_{xj}). These SEs, when all are executed, lead to delivery of power to consumer. A DOS may be written as

$$\mathrm{DOS}_j = \mathrm{se}_{x1}, \mathrm{se}_{x2}, \mathrm{se}_{x3}, \ldots, \mathrm{se}_{xn} \tag{13}$$

where se_{x1}, se_{x1}, $\mathrm{se}_{x2}, \ldots \mathrm{se}_{xn}$ are a set of service events, a DOS_j is a given DOS**.**

DOSP is the possibility of a given DOS on an SE-to-SE basis. It is necessary to define a new matrix to indicate whether a sequence of SEs can realize a DOS (possibility) or not. The possibility can be captured in the following two binary matrices for each DOS.

1) Delivery of service conversion possibility matrix (DOSCPM): For a given DOS_j, a binary matrix CPM_i of size $n(\mathrm{se}_j) \times n(P_c)$ whose entry is equal to one if the SE realizes the conversion process.
2) Delivery of service transmission possibility matrix (DOSTPM): For a given DOS_j, a binary matrix TPM_i of size $1 \times n(P_T)$ whose entry is equal to one if the SE realizes the transmission process.

From these definitions, the conversion and transmission service event matrices for a given DOS_j are respectively, expressed as [49]

$$\mathrm{SE\_}C_{xi} = \left[\mathbf{1}^{n\,(CA)} \mathrm{se}_x^T \mathrm{CPM}_i\right]^T \tag{14}$$

$$\mathrm{SE\_}T_i = \left[\mathbf{1}^{n(A)} \mathrm{Kron}(\mathrm{TPM}_i, \mathbf{1}^{n(T.P)T})\right]^T \tag{15}$$

where Kron is the Kronecker tensor product, and $\mathbf{1}^n$ is a column ones vector with length n. The conversion and transmission service event matrices should be combined together via

$$\mathrm{SE}_{xi} = \left[\frac{\mathrm{SE\_}C_{xi} \;\mid\; \mathbf{0}}{\mathrm{SE\_}T_i}\right]. \tag{16}$$

By the appropriate replacement of $\mathrm{SE\_}C_{xi}$ or $\mathrm{SE\_}T_i$ with zero matrices in (16), the conversion and transmission service event matrices can be calculated as follows:

$$\mathrm{SE}_{C_{xi}} = \left[\frac{\mathrm{SE\_}C_{xi} \;\mid\; \mathbf{0}}{\mathbf{0}}\right] \tag{17}$$

$$\mathrm{SE}_{T_i} = \left[\frac{\mathbf{0} \;\mid\; \mathbf{0}}{SE\_T_i}\right]. \tag{18}$$

D. Proposed Resilience Index

The previous background allows for the introducing a proper resilience index for power grids which is based on full enumeration of possibility paths for each DOS. For this purpose, a sequence of events must occur in power grids, continuously. Actually, electrical power must be generated at a power plant through conversion events, and then is transmitted through transmission lines with transmission events via one or more successive transmission events. Finally, in order to deliver power to a load, the successive transmission events end to the load through conversion events. For any reason, if any of these consecutive events do not occur, the power transmission process from a power plant to an electrical load would not be done in a fair and reasonable manner and as a consequence, power grid resilience decreases. In order to quantify the resilience index, it is necessary to define path enumeration in terms of three types of SCQOF as follows [50].

1) A transmission event follows a conversion event that can be assessed as

$$\begin{aligned}\mathrm{SM}_{CT_{xi}} = \Big[&[\mathrm{SE}_{C_{xi}} \mathrm{RM}_{C_{n\_s}}(1-\mathrm{CM}_{C_{n\_s}})]^V \\ &\times [\mathrm{SE}_{T_i} \mathrm{RM}_{T_{n\_s}}(1-\mathrm{CM}_{T_{n\_s}})]^{VT}\Big] \\ &\times [1-\mathrm{CM}_s]\,.\end{aligned} \tag{19}$$

2) Two successive transmission events that can be evaluated as

$$\begin{aligned}\mathrm{SM}_{TT_i} = \Big[&[\mathrm{SE}_{T_i} \cdot \mathrm{RM}_{T_{n\_s}}(1-\mathrm{CM}_{T_{n\_s}})]^V \\ &\times [\mathrm{SE}_{T_i} \mathrm{RM}_{T_{n\_s}}(1-\mathrm{CM}_{T_{n\_s}})]^{VT}\Big]\,. \\ &\times [1-\mathrm{CM}_s]\end{aligned} \tag{20}$$

3) A conversion event follows a transmission event that can be checked through

$$\begin{aligned}\mathrm{SM}_{TC_{(x+1)i}} = \Big[&[\mathrm{SE}_{T_{(x+1)i}}\mathrm{RM}_{T_{n\_s}}(1-\mathrm{CM}_{T_{n\_s}})]^{V} \\ &\times[\mathrm{SE}_{C_{(x+1)i}}\mathrm{RM}_{C_{n\_s}}(1-\mathrm{CM}_{C_{n\_s}})]^{VT}\Big] \\ &\times[1-\mathrm{CM}_{s}]\end{aligned} \tag{21}$$

where *x* and *x + 1* are the indices of sequential service events, and *i* indicates a specified DOS. In the above-stated equations, RM_{Cn_s} and RM_{Tn_s} can be calculated by the appropriate replacement of RM_C or RM_T with zero matrices in (8). Similarly, CM_{Cn_s} and CM_{Tn_s} can be calculated by the appropriate replacement of CM_C or CM_T with zero matrices in (9).

To determine the number of possible paths for DOS_i, (19)–(21) should be multiplied together via

$$\mathrm{SM}_i = \sum_{p=1}^{P} \mathrm{SM}_{CT_{xi}}\left((\mathrm{SM}_{TT_i})^{p}\right)\mathrm{SM}_{TC_{(x+1)i}} \tag{22}$$

where p is number of possible paths for each of DOS. The sequential constructional grid relation matrix (SM_i) represents the summation of possible paths over *p*. The ratio between the numbers of possible paths before disruption unfold (normal operation conditions) and after that can be assumed as a resilience index. Equation (22) does not consider some of the important power grid problems such as loads and generators capacities, loads and generator priorities, and transmission lines congestion.

The factors that should be considered in the processes of generation and delivering power are power rating of generators and some predetermined priority based on the importance of a load or generator. Furthermore, there is some restriction of delivering power to loads due to the capacity limitation of transmission lines (congestion). To address these limitations, a new and modified resilience index is proposed as in (23), shown at the bottom of this page, where *bin*[] is a binary function that returns "one" for all positive values, and returns "zero" otherwise, subscript *i0* shows normal conditions (before disruption unfold), $\mathrm{LC}_i(\upsilon_1,\upsilon_2)$ is the delivering power to ith load, W_i and W_j are the load and generator weighting factor, respectively, for a given DOS_i. Indeed, coefficients W_i and W_j cover loads and generator priorities. The effect of transmission lines congestion is also considered by the dc OPF problem via $\mathrm{LC}_i(\upsilon_1,\upsilon_2)$. The new index is normalized and fall in between 0 and 1. The Zero value represents the least resilience, and the unit value shows the maximum. It is worth noting that the proposed index calculates the power grid resilience at each time unit (e.g., hour). In order to evaluate power grid resilience over a period of time, the area under the resilience curve versus time should be determined. As the maximum value of the proposed index is equal to the supplied power, the area below the curve represents total amount of supplied energy by the network.

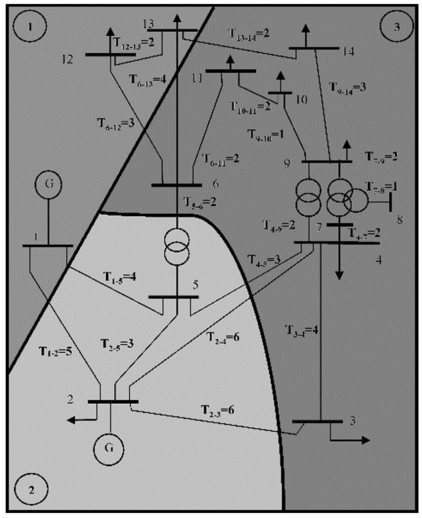

Fig. 4. Single-line diagram of the IEEE 14-bus system including weather regions.

It is of vital need to determine the difference between trigger events and root causes in resilience evaluation. The root causes define the origins and the most basic causes for a severe event (such as limited understanding of the system, deficient vegetation management, and complexity and tight coupling), whereas the trigger events represent the reason for the start of that event (winds, flood, earthquake, etc.). Since in the proposed index, the ratio between the numbers of feasible paths before and after disruption unfold is considered, this index ignores root causes and only reflects the trigger events. Root causes analysis is a structural procedure and used for recognition the failure causes and its effects. This procedure helps prevent the failure reoccurring and consequences and consequently enhance the network resilience.

III. Results and Discussions

This section presents the proposed resilience evaluation approach, with the impact modelling of severe windstorm on a modified version of the IEEE 14-bus system. The modified network (shown in Fig. 4) consists of 20 lines and 14 buses, including 2 generator buses and 10 load buses. The grid has both HV and MV networks [51]. Without loss of generality, the length of all lines is assumed 1 km. Number of towers for each line is shown in Fig. 4.

The following assumptions are considered.

1) A simulation period of three days is selected (i.e., 72 h). The number of Monte Carlo samples is 100.
2) The IEEE 14-bus power system is arbitrarily divided into three weather regions (see Fig. 4) to model the regional impact of the wind event. The assumed reliability data

$$RI = \frac{\sum_{j=1}^{n(G)}\sum_{i=1}^{n(\mathrm{DOS})}\sum_{\upsilon_1=1}^{n(\mathrm{row})}\sum_{\upsilon_2=1}^{n(\mathrm{column})} W_j \times W_i \times \mathrm{LC}_i(\upsilon_1,\upsilon_2)\frac{\mathrm{SM}_i}{\mathrm{SM}_{i0}}}{\sum_{j=1}^{n(G)}\sum_{i=1}^{n(\mathrm{DOS})}\sum_{\upsilon_1=1}^{n(\mathrm{row})}\sum_{\upsilon_2=1}^{n(\mathrm{column})} W_{j0} \times W_{i0} \times \mathrm{LC}_{i0}(\upsilon_1,\upsilon_2)\mathrm{bin}\left[\mathrm{SM}_i\right]} \tag{23}$$

TABLE I
RELIABILITY DATA OF LINES AND TOWERS IN EACH REGION

	R_1	R_2	R_3
Line Failure Rate (occ/hr)	0.015	0.02	0.01
Line Repair Time (hr)	10	12	15
Tower Repair Time (hr)	50	60	75

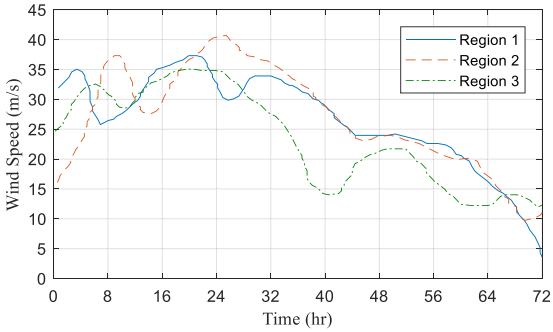

Fig. 5. Hourly regional wind profiles.

of towers and lines for each weather region are shown in Table I.

3) Hourly regional wind profiles were generated randomly at different locations and presented in Fig. 5.
4) When a transmission line encounters two weather regions and experiencing different wind conditions in each region, the worst weather condition is considered.
5) The generator weighting factors to be the same.
6) All the generation units are resilient in exposure to wind.
7) Before disruptions unfold, the NSCGCM is initially set to zero ($\mathrm{CM}_{n\_s} = \mathbf{0}$).
8) The SCGCM (CM_s) has the minimal constraints based on the relationship between input and output events.
9) As the number of generators and loads are 2 and 11 in the simulated network, respectively, the number of the delivery of power from each generator to each load (DOS) is equals to 22.

Based on these assumptions, RM_C, RM_T, RM_{n_s} and CPMs for each DOS are then calculated. First, all load importance factors are assumed to be the same. The resilience indices for two different cases are calculated: both lines and towers failures are considered [see Fig. 6(a)] and only lines failures are taken into account [see Fig. 6(b)]. As expected, the figures show that when towers failures are taken into account, the power grid resilience is greatly reduced.

The area under the resilience curve versus time represents the total amount of supplied energy by the network. If difference between the two mentioned indices ($35.6360 - 33.4573 = 2.1787$) are calculated and then it is converted to the amount of supplied energy by the network, this is equivalent to 564.3 MWh. This amount of energy is so considerable.

It is worth noting that RI value is the mean value of the N Monte Carlo estimated values. For more clarity, the standard deviation and the coefficient of variation (CV) are also shown in

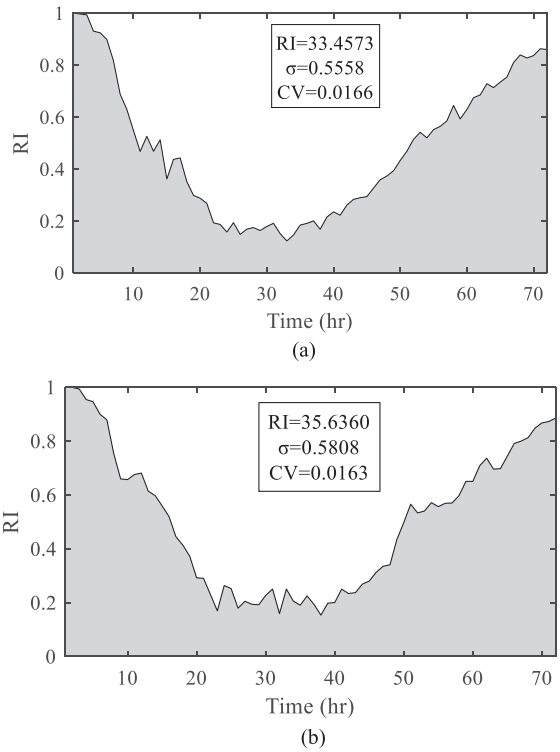

Fig. 6. Grid resilience index with the standard deviation (σ) and the CV (a) when both line and towers failures are considered and (b) when only lines failures are included.

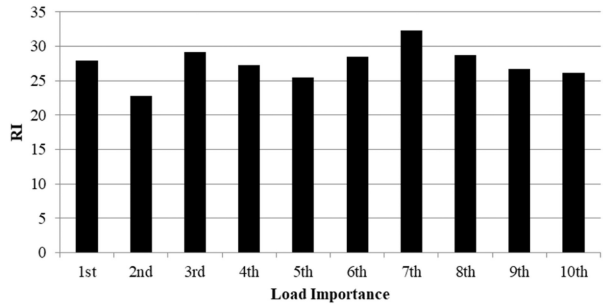

Fig. 7. Comparison of the proposed resilience index under different critical loads.

Figs. 6(a) and (b). As shown in the figures, these values are very small and this shows that all data are close to the mean value of RI. In spite of this, the calculated resilience indices have been verified by the adequate hypothesis test.

To illustrate the effect of loads priority in grid resilience, weighing factor of one of the loads (critical load) is assumed to be higher than the other loads and the proposed resilience index is calculated. This is done for each of the load and the results are shown in Fig. 7. As it can be seen, when the loads importance is taken into account, the overall system resilience index may change due to factors such as wind speed profile in various regions and different lines and towers failure rates and repair times. The figure shows that when the load #2 is a critical load, the grid is in its least resilience value. This is because the load #2 is the largest load and this load is supplied from the lines that are all located in region 3. This region has the longest

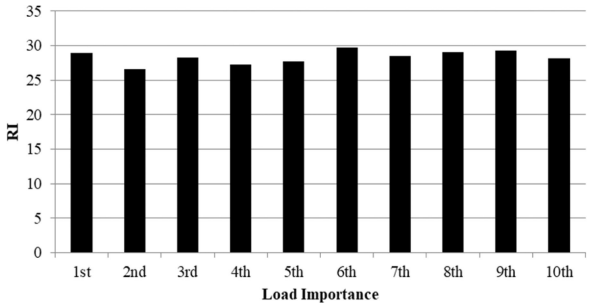

Fig. 8. Effect of the redundancy enhancement strategy on power grid resilience.

line repair time. Also, these lines have a significant number of towers. As a result, value of resilience is considerably reduced.

On the other hand, if the loads located in MV network are chosen as the critical load, since it can be supplied by several DOSs (which includes lines with a low number of towers), the proposed resilience index goes higher.

In order to show the effect of wind speed profile on the power grid resilience, the hourly wind profiles in Fig. 5 are scaled up by 1.4 and then the proposed resilience index is calculated. The new resilience value is 7.8706. It is evident that the higher the wind speed, the smaller the grid resilience.

Remedial actions have positive impact on grid resilience enhancement. In order to show the impact of remedial actions on the grid resilience, the following actions are considered: adding one transmission line in parallel with the most critical line and decreasing repair time using the same multiplication factor for all lines and towers.

As the line 5–6 connects the HV and MV networks by only one transformer, its failure has the greatest impact on the network behavior. Therefore, a transformer with the same ratings is added between the buses #5 and #6. Fig. 8 shows the proposed resilience index with different critical loads when a redundant path is added between the buses #5 and #6. As shown, by applying this remedial action, the overall grid resilience increases. It should be noted that the resilience after adding the redundant path resulted in resilience reduction for some loads, such as third, seventh, and eleventh. The system resilience index depends on some factors such as wind speed profile in various regions and different lines and towers failure rates and repair times. All the three mentioned loads have the longest repair time. Also, since the main path for supplying these loads is the line 2–4 and adding a parallel line with line 5–6 has no effect on this path, the reduction in resilience for these loads is reasonable. The overall grid resilience was calculated based on average of all loads. The overall grid resilience in Fig. 8 is equivalent to 28.165 and in Fig. 7 is equivalent to 27.791.

The effect of repair time on grid resilience is also demonstrated in Table II. The table reveals that the grid resilience significantly decreases as the repair time is increased.

As mentioned in the introduction, limited studies where reported deal with comprehensive resilience Index. However, in [23], a resilience assessment approach was introduced for power system through three independent periods; before, during, and after disaster unfold. For comparison of the index of [23] with

TABLE II
EFFECT OF REPAIR TIME ON GRID RESILIENCE

Repair Time Factor	0.8	1	2	5
Power Grid Resilience	38.9402	33.4573	20.8848	16.9978
CV	0.0158	0.0166	0.0267	0.0323

the index of this article, some simplifying assumptions must be made which are as follows.

1) There is only one weather region in the studied area.
2) Hourly regional wind profiles were not considered in [23]. So, the wind speed is assumed constant over time and equal to 38 m/s (the value which was chosen in [23]).
3) All the towers are assumed to be resilient in exposure to wind event and only transmission lines failures are considered. Furthermore, it is assumed that only three lines may be failed, including lines 1–5, 2–4, and 5–6.
4) The simulation does not consider loads and generators priorities during assessment of the grid resilience (as in [23]).
5) Equation (14) in [23] (CLLP) is used for comparison with our index (RI)

$$\text{CLLP} = \frac{\sum_{b=1}^{N_b} (L_{nl,b} - L_{dl,b})}{\sum_{b=1}^{N_b} L_{nl,b}} = 0.1528. \qquad (24)$$

Our resilience index can be calculated as in (23): RI = 0.8472, and we have RI = *1*–CLLP = 1–0.1528 = 0.8472 as expected.

IV. CONCLUSION

In order to evaluate and quantify the resilience of power grids, a novel matrix-based approach is introduced. For this purpose, first, the disaster modeling is illustrated. Then, the approach is followed by the impact modeling of severe weather conditions on the transmission grids. The impact is modeled with the fragility curves based on reliability data and using the Monte Carlo simulations method. Finally, a novel systematic resilience matrix-based index was suggested that considers the loads and generator priorities and transmission lines congestion. The proposed approach is tested on the IEEE 14-bus system and the resilience index is calculated under different conditions. The index presented in this article has also described and demonstrated the effect of various remedial actions.

Although the proposed method may have similarities with traditional graph theory, such as shortest path length, but there are some major differences. For example, this approach considers the explicit description of multiple transmission nodes and assets with multiple conversion processes. The presented approach would help the power grid operators and asset investment manager to prepare against natural disasters. The identified resilience measure would take the lead in planning, robustness, and hardening of the power system. Future works can be on the development of new formulations considering type of transmission process, storage resources, and various types of ac and dc loads that are compatible with the proposed approach.

REFERENCES

[1] U.S.–Canada Power System Outage Task Force, "Final report on the August 14, 2003 blackout in the United States and Canada: Causes and recommendations," U.S. Dept. Energy, Washington, DC, USA, Tech. Rep., Apr. 2004.

[2] UCTE, "Interim report of the investigation committee on the 28 September 2003 blackout in Italy," Brussels, Belgium, Tech. Rep., Oct. 2003.

[3] UCTE, Final report system disturbance on 4 November 2006, Brussels, Belgium, 2007.

[4] FERC and NERC, *Arizona–Southern California Outages on September 8, 2011: Causes and recommendations*," Washington, DC, USA, Apr. 2012.

[5] S. Hosseini, K. Barker, and J. E. Ramirez-Marquez, "A Review of definitions and measures of system resilience," *Rel. Eng. Syst. Saf.*, vol. 145, pp. 47–61, 2016.

[6] G. A. Bonanno, S. Galea, A. Bucciarelli, and D. Vlahov, "What predicts psychological resilience after disaster? The role of demographics, resources, and life stress," *J. Consulting Clin. Psychol.*, vol. 75, no. 5, pp. 671–82, Oct. 2007.

[7] S. Jackson and TL. Ferris, "Resilience principles for engineered systems," *Syst. Eng.*, vol. 16, no. 2, pp. 152–164, Jun. 2013.

[8] A. Gholami, F. Aminifar, and M. Shahidehpour, "Front lines against the darkness: Enhancing the resilience of the electricity grid through microgrid facilities," *IEEE Electrific. Mag.*, vol. 4, no. 1, pp. 18–24, Mar. 2016.

[9] L. Yong and C. Singh, "A methodology for evaluation of hurricane impact on composite power system reliability," *IEEE Trans. Power Syst.*, vol. 26, no. 1, pp. 145–152, Feb. 2011.

[10] M. Panteli and P. Mancarella, "Modeling and evaluating the resilience of critical electrical power infrastructure to extreme weather events," *IEEE Syst. J.*, vol. 11, no. 3, pp. 1733–1742, Sep. 2017.

[11] R. Billinton, *Power System Reliability Evaluation*. New York, NY, USA: Taylor & Francis, 1970.

[12] *Terms For Reporting And Analyzing Outages Of Electrical Transmission And Distribution Facilities And Interruptions To Customer Service*, IEEE Standard 346, 1973.

[13] R. Billinton and K. E. Bollinger, "Transmission system reliability evaluation using Markov processes," *IEEE Trans. Power App. Syst.*, vol. PAS-87, no. 2, pp. 538–547, Feb. 1968.

[14] H. Liu, R. A. Davidson, and T. V. Apanasovich, "Statistical forecasting of electric power restoration times in hurricanes and ice storms," *IEEE Trans. Power Syst.*, vol. 22, no. 4, pp. 2270–2279, Nov. 2007.

[15] J. Aznarte and N. Siebert, "Dynamic line rating using numerical weather predictions and machine learning: A case study," *IEEE Trans. Power Del.*, vol. 32, no. 1, pp. 335–43, Feb. 2017.

[16] Y. Liu, "Operational statistic risk assessment for power systems under extreme weather conditions," in *Proc. 10th Int. Conf. Adv. Power Syst. Control, Oper. Manage.*, 2015, pp. 80–86.

[17] J. P. Gilly, M. Kechidi, and D. Talbot, "Resilience of organizations and territories: The role of pivot firms," *Eur. Manage. J.*, vol. 32, no. 4, pp. 596–602, 2014.

[18] R. L Martin, "Regional economic resilience, hysteresis and recessionary shocks," *J. Econ. Geogr.*, vol. 12, pp. 1–32, 2012.

[19] R. Faturechi and E. Miller-Hooks, "Travel time resilience of roadway networks under disaster," *Transp. Res. Part B, Methodol.*, vol. 3, pp. 47–64, 2014.

[20] R. Faturechi, E. Levenberg, and E. Miller-Hooks, "Evaluating and optimizing resilience of airport pavement networks," *Comput. Oper. Res.*, vol. 43, pp. 335–48, 2014.

[21] R. Pant, K. Barker, and C. W. Zobel, "Static and dynamic metrics of economic resilience for interdependent infrastructure and industry sectors," *Rel. Eng. Syst. Saf.*, vol. 125, pp. 92–102, 2014.

[22] D. G. Dessavre, J. E. Ramirez-Marquez, and K. Barker, "Multidimensional approach to complex system resilience analysis," *Rel. Eng. Syst. Saf.*, vol. 149, pp. 34–43, 2016.

[23] H. Zhang, H. Yuan, G. Li, and Y. Lin, "Quantitative resilience assessment under a Tri-stage framework for power systems," *Energies*, vol. 11, no. 6, Jun. 2018, Art. no. 1427.

[24] M. Panteli, C. Pickering, S. Wilkinson, R. Dawson, and P. Mancarella, "Power system resilience to extreme weather: Fragility modeling, probabilistic impact assessment, and adaptation measures," *IEEE Trans. Power Syst.*, vol. 32, no. 5, pp. 3747–3757, Sep. 2017.

[25] G. Fu G *et al.*, "Integrated approach to assess the resilience of future electricity infrastructure networks to climate hazards," *IEEE Syst. J.*, vol. 12, no. 4, pp. 3169–3180, Dec. 2018.

[26] P. Wood, D. Shiltz, T. R. Nudell, A. Hussain, and A. M. Annaswamy, "A framework for evaluating the resilience of dynamic real-time market mechanisms," *IEEE Trans. Smart Grid*, vol. 7, no. 6, pp. 2904–12, Nov. 2016.

[27] M. Panteli, D. N. Trakas, P. Mancarella, and N. D. Hatziargyriou, "Boosting the power grid resilience to extreme weather events using defensive islanding," *IEEE Trans. Smart Grid*, vol. 7, no. 6, pp. 2913–22, Nov. 2016.

[28] H. Farzin, M. Fotuhi-Firuzabad, and M. Moeini-Aghtaie, "Enhancing power system resilience through hierarchical outage management in multi-microgrids," *IEEE Trans. Smart Grid*, vol. 7, no. 6, pp. 2869–79, Nov. 2016.

[29] A. Azadeh, V. Salehi, M. Arvan, and M. Dolatkhah, "Assessment of resilience engineering factors in high-risk environments by fuzzy cognitive maps: A petrochemical plant," *Safety Sci.*, vol. 68, pp. 99–107, 2014.

[30] M. J. Alenazi, "Graph resilience improvement of backbone networks via node additions," in *Proc. 8th Int. Workshop Resilient Netw. Des. Model.*, 2016, pp. 231–237.

[31] A. Gholami, T. Shekari, M. H. Amirioun, F. Aminifar, M. H. Amini, and A. Sargolzaei, "Toward a consensus on the definition and taxonomy of power system resilience," *IEEE Access*, vol. 6, pp. 32035–32053, 2018.

[32] A. Hussain, V. H. Bui, and H. M. Kim, "Resilience-oriented optimal operation of networked hybrid microgrids," *IEEE Trans. Smart Grid*, vol. 10, no. 1, pp. 204–215, Jan. 2019.

[33] M. Panteli, P. Mancarella, D. N. Trakas, E. Kyriakides, and N. D. Hatziargyriou, "Metrics and quantification of operational and infrastructure resilience in power systems," *IEEE Trans. Power Syst.*, vol. 32, no. 6, pp. 4732–42, Nov. 2017.

[34] E. Hollnagel, D. D. Woods, and N. Leveson, *Resilience Engineering: Concepts and Precepts*. Ashgate Publishing, 2007.

[35] A. M. Madni and S. Jackson, "Towards a conceptual framework for resilience engineering," *IEEE Syst. J.*, vol. 3, no. 2, pp. 181–191, Jun. 2009.

[36] R. Pant, K. Barker, and C. W. Zobel, "Static, and dynamic metrics of economic resilience for interdependent infrastructure, and industry sectors," *Rel. Eng. Syst. Saf.*, vol. 125, pp. 92–102, May 2013.

[37] Y. Liu, S. Li, P. W. Chan, and D. Chen, "Empirical correction ratio and scale factor to project the extreme wind speed profile for offshore wind energy exploitation," *IEEE Trans. Sustain. Energy*, vol. 9, no. 3, pp. 1030–40, Jul. 2018.

[38] M. I. Garcia-Planas and T. Gongadze, "Wind profile prediction using linear markov chains: A linear algebra approach," *IEEE Latin Amer. Trans.*, vol. 16, no. 2, pp. 536–41, Feb. 2018.

[39] F. Casciati and L. Faravelli, *Fragility Analysis of Complex Structural Systems*. Taunton, U.K.: Res. Studies Press, 1991.

[40] N. D. Trakas, M. Panteli, and N. D. Hatziargyriou, "Spatial risk analysis of power systems resilience during extreme events," *Int. J. Risk Anal.*, vol. 39, no. 1, pp. 195–211, 2019.

[41] R. Billinton and R. N. Allan, *Reliability Evaluation of Power Systems*. New York, NY, USA: Plenum, pp. 400–405, 1996.

[42] K. Xie, J. Zhou, and W. Li, "Analytical model and algorithm for tracing active power flow based on extended incidence matrix," *Elect. Power Syst. Res.*, vol. 79, no. 2, pp. 399–405, 2009.

[43] C. Perrow, *Charles, Normal Accidents: Living With High Risk Technologies*. Princeton, NJ, USA: Princeton Univ. Press, 1999.

[44] O. L. DeWeck, D. Roos, and C. L. Magee, *Engineering Systems: Meeting Human Needs in A Complex Technological World*. Cambridge, MA, USA: MIT Press, 2011.

[45] A. M. Farid, "Static resilience of large flexible engineering systems: axiomatic design model and measures," *IEEE Syst. J.*, 2015.

[46] A. M. Farid, "Static resilience of large flexible engineering systems: Part I—Axiomatic design model," in *Proc. 4th Int. Eng. Syst. Symp.*, Hoboken, NJ, USA, 2014, pp. 1–8.

[47] A. M. Farid, "Static resilience of large flexible engineering systems: Part II—Axiomatic design measures," in *Proc. 4th Int. Eng. Syst. Symp.*, Hoboken, NJ, USA, 2014, pp. 1–8.

[48] A. M. Farid and D. C. McFarlane, "Production degrees of freedom as manufacturing system reconfiguration potential measures," *Proc. Inst. Mech. Eng., Part B, J. Eng. Manuf.*, vol. 222, no. 10, pp. 1301–1314, 2008.

[49] A. M. Farid, Reconfigurability measurement in automated manufacturing systems, Ph.D. dissertation, Dept. Eng., Inst. Manuf., Univ. Cambridge, Cambridge, U.K., 2007.

[50] A. M. Farid, "Product degrees of freedom as manufacturing system reconfiguration potential measures," *Int. Trans. Syst. Sci. Appl.*, vol. 4, no. 3, pp. 227–242, 2008.

[51] [Online]. Available: http://www.ee.washington.edu/research/pstca/